Thin-Walled Structures 84 (2014) 226–240

Contents lists available at ScienceDirect

Thin-Walled Structures

journal homepage: www.elsevier.com/locate/tws

Wind buckling of tanks with conical roof considering shielding by another tank

Carlos A. Burgos [a], Rossana C. Jaca [a], Jorge L. Lassig [a], Luis A. Godoy [b,c,*]

[a] Engineering School, Universidad Nacional del Comahue, Neuquén, Argentina
[b] FCEFyN, Universidad Nacional de Córdoba, Córdoba, Argentina
[c] Science and Technology Research Council (CONICET), Argentina

ARTICLE INFO

Article history:
Received 19 April 2014
Received in revised form
10 June 2014
Accepted 18 June 2014

Keywords:
Buckling
Group effects
Shells
Tanks
Wind loads

ABSTRACT

Oil storage tanks are usually arranged in groups in tank farms, and this configuration may affect their buckling and postbuckling strength under wind loads. The assessment of wind action on tank structures is performed in this work by means of wind tunnel experiments to evaluate the pattern of pressure distribution for a tank which is shielded by another tank under various configurations and separation between them. The experimental results show significant changes in pressures due to shielding effects. In a second stage the structural response under the pressures previously evaluated is performed by finite element analysis using both linear bifurcation and geometrically nonlinear analysis. Results of two-tank interaction are compared with those of an isolated tank. Based on the results, it is concluded that the changes in wind pressures due to group effects induce changes in buckling loads and in the associated deflected patterns.

1. Introduction

Short steel tanks are usually employed in the oil industry to store large volumes of fluid, with aspect ratios between $0.2 < H/D < 1.0$ in which H is the height of the cylindrical part and D is the diameter; however, frequently employed dimensions have aspect ratios between 0.2 and 0.6. Tanks may have an internal floating roof and a fixed roof (either conical, flat, or dome roof). Some tanks do not have a fixed roof so that the floating roof is directly exposed to the environment.

Oil tanks are frequently constructed in groups in what are known as tank farms. Farms include between tens and hundreds of tanks, which may be the property of one or several oil companies. Under strong winds, the structural behavior of tanks depends on their location within the group, so that it may be possible to distinguish between tanks located in a front line from those placed in a second or third line with respect to the perimeter of the facility.

Because tank farms are so common in oil facilities, it is surprising to find that most available information on the wind response of tanks concentrates on isolated tanks in flat terrain. This is evidenced in the American [2] and European [5] recommendations for the design of aboveground tanks, in which only the behavior of isolated shells is considered in detail.

The first investigation on the interaction between neighboring cylinders with a roof was perhaps published by Esslinger et al. [4] in Germany, in which wind tunnel tests were reported on two small-scale silos with similar dimensions. The models were placed in a line with the wind direction, with dimensions which were representative of tall silos with $H/D > 2$. For even taller structures, with $H/D > 10$, Zdravkovich [28] and Tsutsui et al. [22] studied the interaction between two aligned cylinders. More recent studies concerning pressures in shells which are localized close to each other under wind were published by Gu and Sun [6] and Orlando [12]. However, such studies are not relevant to explain interaction effects between oil storage tanks, which are short cylinders with relative dimensions in the order of $0.25 < H/D < 0.5$.

A wind tunnel investigation on silos placed very close to each other in a line perpendicular to the direction of wind was carried out in Australia in the 1970s by Vickery and Ansourian [24]. The results have been reported in the form of an analytical expression for pressure coefficients around the circumference in the European recommendations [18], but without reference to the dimensions and separation between the shells.

Wind tunnel studies have been made of the external pressure distributions on multiple circular cylinders with conical or flat roofs. Regarding wind tunnel studies of tanks, MacDonald et al.

* Corresponding author at: FCEFyN, Universidad Nacional de Córdoba, Córdoba, Argentina.
E-mail address: lgodoy@efn.uncor.edu (L.A. Godoy).

http://dx.doi.org/10.1016/j.tws.2014.06.007
0263-8231/

[10] concluded that pressure distributions are independent of Reynolds number provided $Re > 1 \times 10^4$. Sabransky and Melbourne [19] studied silo structures with aspect ratios $H/D=0.66$ and conical roof inclination angle of 27°.

MacDonald et al. [11] performed wind tunnel testing of five tanks in a line in which the blocking and the target tank models had both a flat roof; however, only those in tandem configuration are reviewed here because they can be compared with present results. For point pressure measurements, a configuration with $S=0.125D$ was tested, where S is the wall-to-wall minimum distance between tanks. Mean value pressures showed two lobes of positive pressures centered with respect to the windward meridian, each with a central angle of approximately 50°. The positive pressures resulted in values significantly lower than in the isolated tank, with pressure coefficients $C_p < 0.5$. Peak suctions (located at 90° from the windward meridian) were also smaller, with $C_p < 1.0$. The single case investigated does not allow understanding effects due to tank separation. Panel measurements, on the other hand, were studied for configurations at $S=0.125D$, $0.25D$, and $0.5D$. The results for $S=0.5D$ are shown in the paper.

Tanks located in a second line with respect to the periphery of a tank farm, in which the blocking tank had a flat roof and the target tank had a conical roof, were studied by Portela and Godoy [13] based on wind tunnel tests. Six configurations were tested, with changes in the separation between tanks ($S=0.5D$ and $S=1.0D$) and in the relative height between blocking and target tank. Other cases reported include two tanks in the first line blocking the flow of a tank in a second line, with separations $S=0.5D$ and $S=1.0D$. Contours of pressure coefficient were presented and subsequently employed to carry out linear bifurcation analysis (LBA) and geometrically nonlinear analysis (GNA) on the tanks for which measurements were taken, always in the second line with respect to the periphery of the tank farm; results were compared with those obtained for an isolated tank [14]. Case studies concerning six tanks in a small plant were investigated in Ref. [15] in wind tunnel to obtain pressure coefficients for one target tank under various wind directions; LBA buckling and GNA post-buckling were next computed. Iamandi et al. [7] performed wind tunnel testing of a four-tank configuration due to an accident in a small chemical storage station in Romania but did not provide pressure coefficients.

Tall cylinders ($H/D=2.56$) with flat roof in tandem arrays were studied by Said et al. [20] by means of wind tunnel tests and finite volume simulations. The flow pattern was found to be highly dependent on the separation S between both cylinders: for the short separation $S=1.28D$, the flow accelerates on the roof of the first cylinder and impacts on the top part of the second cylinder, while increasing the pressure. The wake of the first cylinder modifies the pressure field on the target tank and reduces the pressures on the windward region. This effect decreases as the distance increases to $S=5.12D$, with the consequence that the target tank becomes subjected to a flow pattern that is similar to that in the isolated tank.

Uematsu and coworkers [23,25] reported wind tunnel results on open top tanks to investigate group effects in arrangements of two, three and four tanks. The tanks had the same geometry with aspect ratios of $H/D=0.25D$, $0.5D$, and $1.0D$ and spacings of $0.125D < S < 1.0D$. Zhao et al. [27] were also interested in large open-topped tanks with low aspect ratio ($H/D=0.275$), and performed a comprehensive wind tunnel study considering two, three, and four interacting tanks, all of which were instrumented. Two tanks of identical geometry in tandem configuration were tested at $S=0.5D$, $1.0D$, and $1.5D$. Pressures on the external wall of the second tank showed large changes, with peak positive pressures in the windward region for $S=0.5D$ being reduced to 0.24 of their values in the isolated tank; whereas less significant reductions were obtained for larger values of S. Changes were found not only in pressure values but also in pressure distributions. Reductions in pressures on the internal walls were also reported in the windward region. The results highlight the expected changes in pressures for open tanks, but the results cannot be directly employed for tanks having a fixed roof.

The diversity of configurations which may be found in tank farms, even for tanks having similar dimensions and spaced in a regular pattern, points to the need to have more information on pressure coefficients and on the structural response to such wind. This work addresses the problem of a tank with conical roof which is obstructed by another one having the same geometry, in which the angle of wind incidence is taken as a variable to investigate several group configurations. Wind tunnel studies are performed to obtain pressure coefficients, which are subsequently employed in a finite element analysis of shell buckling. Two approaches of shell buckling are investigated, namely linear bifurcation analysis (LBA) and geometrically nonlinear analysis with imperfections (GNIA).

2. Wind tunnel experiments

2.1. Main features of the wind tunnel facility

The wind tunnel facility at the National University of La Plata, which is the largest facility in its kind in Argentina, has been used in this research. The tunnel is capable of reproducing an atmospheric boundary layer, in which high turbulence may be generated together with a non-uniform wind velocity in elevation.

Fig. 1 shows the main components of this close-circuit wind tunnel, with a cross section having 1.40 m (width), 1.0 m (height), and 7.5 m in length. The fan has six blades and is moved by a 50 HP engine. The engine has a system of velocity control which allows changing the flow velocity up to a maximum of 20 m/s measured at the center of the cross section. The access door with glass panels to visualize the development of the test is shown in Fig. 1a, whereas the section where testing is done is shown in Fig. 1b.

Air flows through a honeycomb to enforce axial symmetry and through a set of horizontal obstacles (shown in Fig. 1b) which can rotate on their axes to generate turbulence. Changes in turbulence are obtained by means of variations of the relative location of the obstacles with respect to the wind direction. Once the desired turbulence has been obtained, roughness is modeled by small parallelepiped blocks attached to the floor.

The mechanism employed can represent mean velocities in elevation that follow power or logarithmic laws, depending on the needs of the study; in our case the applied power law was adopted with an exponent $P=0.32$. Different types of turbulence may be implemented in the lower atmospheric boundary layer. During testing, the turbulence intensity was 0.15.

The tunnel is equipped with a system of NetScanner electronic pressure sensors with 128 channels, in which pressures are recorded. A computer is connected for the acquisition and processing of experimental data. A hot wire anemometer with telescopic arm is employed to record reference velocity and temperature of flowing air.

2.2. Prototype tanks considered

A specific geometry was chosen as a case study in this research, having $H/D=0.52$; in the prototype, the dimensions are $D=30.48$ m and $H=15.75$ m.

The separation S between tanks in a tank farm is an important parameter in the present study. Because of limitations in available space in an oil facility, there is a trend to locate them as close as

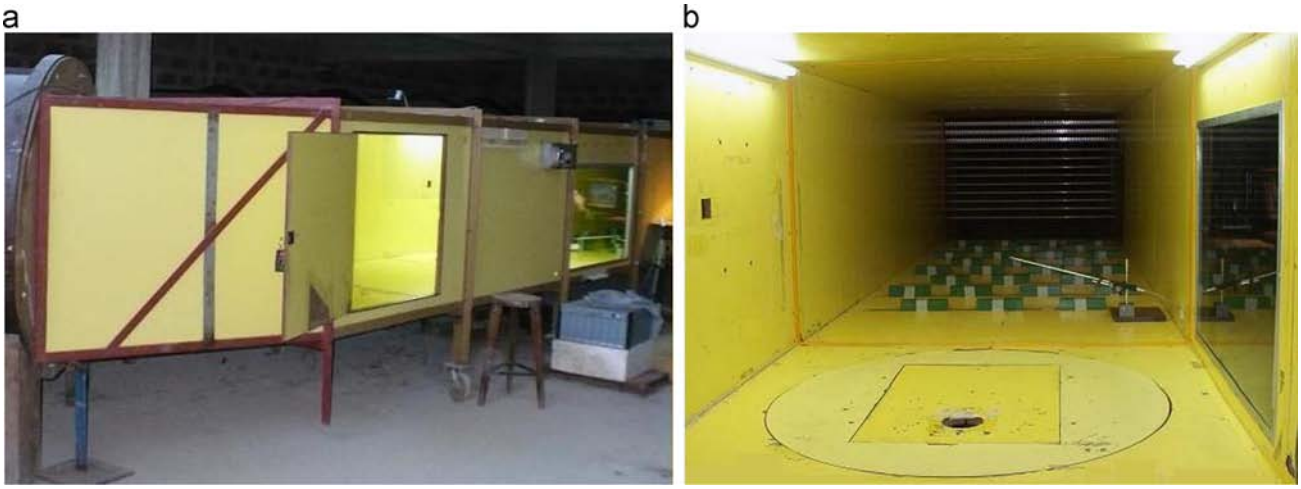

Fig. 1. Wind tunnel at the National University of La Plata in Argentina: (a) external view and (b) internal view of the section where tests are conducted.

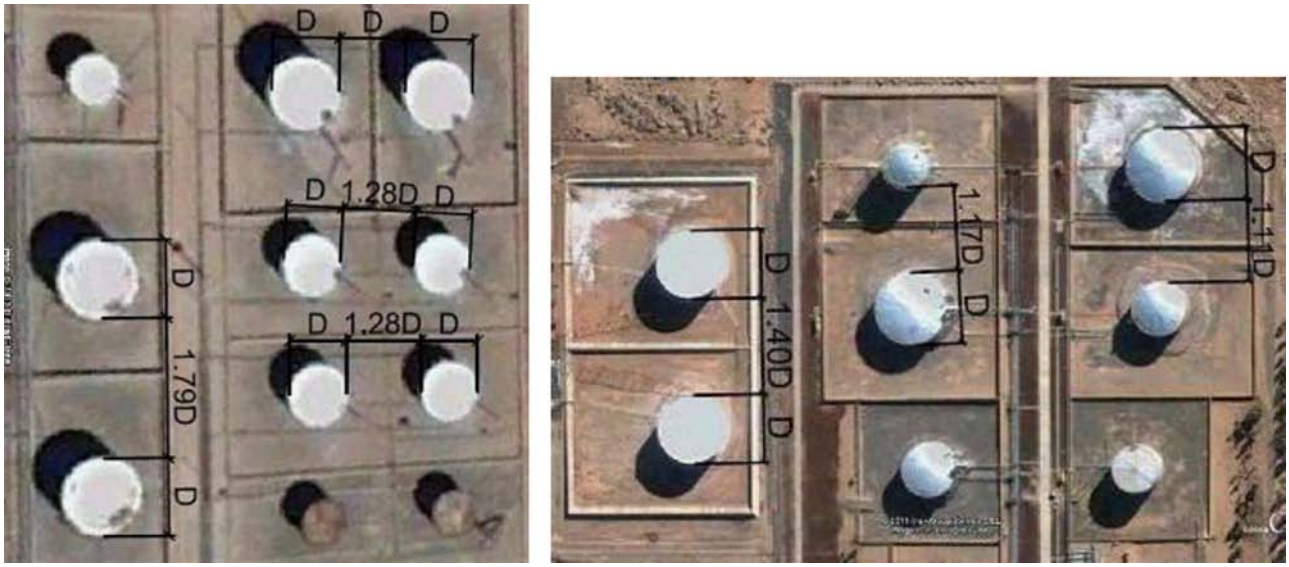

Fig. 2. Groups of tanks in two tank farms located on the Northern part of Patagonia, Argentina.

possible; on the other hand, typical regulations establish a minimum distance between tanks equal to the diameter of the largest tank, measured from wall to wall. There are also limitations regarding the distance to public roads and to other installations.

A survey of aerial photographs of tank farms located in the northern region of Patagonia in Argentina [8] shows that typical separations S between tanks are between 1.0D and 1.8D, as illustrated in Fig. 2. In general terms, tanks are placed in pairs, even though there may be more tanks in the plant. It was decided to perform wind tunnel testing considering two tanks, in which one is the target tank, which is instrumented to obtain pressure coefficients, and the other one (which has not been instrumented in this research) is placed to block the wind flow. Based on observations, the distances between tanks were adopted at $S=1.0D$, $S=1.5D$, and $S=1.8D$.

2.3. Experimental model

The dimensions of the small scale models to be tested in the wind tunnel were chosen by similitude considerations with the prototype discussed previously, and taking into account the main features of the wind tunnel facility in which they were to be tested. To this effect, the most important aspect of the wind tunnel is the cross sectional area of 1.4 m^2. A value of 5% was adopted as maximum relation between model area and cross sectional area to avoid blockage of the flow, as recommended by ASCE [3].

The models were fabricated using a 200 mm diameter PVC tube, thus having a prototype-model relation of $L_r=D_{prototype}/D_{model}=152.4$. Other dimensions in the model are calculated based on L_r, and the dimensions adopted are shown in Table 1. Blocking of the cross section of the tunnel for this model is of only 3.22%, which is smaller than recommended values.

For a reference wind velocity of 17 m/s in the tunnel at elevation 1.74H, the corresponding velocity at 0.92H was 12.63 m/s. The elevation at 0.92H is close to the top of the cylinder and was chosen to identify reference velocities used to evaluate pressure coefficients. This procedure is similar to what was adopted, for example, by MacDonald et al. [10].

The tank tested in the experiments is shown in Fig. 3. Pressure gauges were placed at three elevations in the cylinder (at 0.10H, 0.50H, 0.90H), plus three in the roof (at 1.02H, 1.09H, and 1.15H) and one at the top of the conical roof. In the circumferential direction the gauges were located at 22.5° spacing, with a total of 97 points at which pressures were measured.

There are two models in the experiments, both with the same characteristics, but a bottom plate was present in the blocking

tank whereas no plate was placed at the bottom of the tank in which measurements were taken, because all pressure gauges were conducted on the inside of such model.

2.4. Testing procedure

To simulate shielding and interaction between tanks in a tank farm, two variables were considered: the distance S between tanks and the direction of wind incidence. Separations between tanks $S=1.0D$, $S=1.5D$, and $S=1.8D$ were investigated, with directions characterized by angles ranging between 0° and 90°. The target model was tested in the same position, and the position of the blocking tank was changed to obtain different configurations. Measurements were made at a wind speed of 17 m/s, and pressure and temperature were recorded in each case to adjust the values. The velocity inside the wind tunnel was measured using an anemometer at $1.27H$ from the surface, which is equivalent to 20 m elevation in a real scale.

For separation between tanks $S=1.0D$, for each direction of wind incidence, the flow was stabilized and pressures were measured during one minute. Five directions were considered, as follows: In Configuration C_1, known as tandem array, both tanks are aligned with the direction of wind, so that maximum blockage occurs. Configurations C_2, C_3, C_4 and C_5 were tested with the blocking tank displaced at angles of 22.5°, 45°, 67.5°, and 90°, measured counter-clockwise with respect to the direction of wind incidence. In Configuration C_5 the two tanks are perpendicular to the wind direction to represent tanks located at a first line. A configuration with just an isolated tank, named C_0 has also been studied for reference. Testing for separations $S=1.5D$ and $S=1.8D$ was similar to the above description. Fig. 4 illustrates the scheme of tests with directions of incidence.

Pressure coefficients C_p are defined in the usual way

$$C_p = \frac{p - p_\infty}{(1/2)\rho_\infty V_\infty^2} \quad (1)$$

where ρ_∞ is the fluid density of the unperturbed flow, V_∞ is the flow velocity; and $(p-p_\infty)$ is the difference between the pressure measured in the model and that of the unperturbed flow. The data acquisition system employed records the term $(p-p_\infty)$ directly in units of pressure, with a frequency of data acquisition of 3.5 Hz. The unperturbed density recorded was 1.22 kg/m^3.

Table 1
Geometries of prototype and model.

Prototype			Model		
Diameter D (m)	Cylinder height H (m)	Roof height h (m)	Diameter D' (cm)	Cylinder height H' (cm)	Roof height h' (cm)
30.48	15.75	2.86	20	10.33	1.88

3. Wind tunnel results

3.1. Wind pressures

Pressure contours evaluated from the tests are shown in three-dimensional representations in Fig. 5 for the five configurations investigated and for the isolated tank. Positive values indicate pressures acting on the surface, while negative values indicate suction.

For the tandem array C_1, the peak pressures on the cylinder are displaced towards the roof junction and with values of $C_p=1.15$ which are higher than in the single tank configuration. Pressures on the roof are predominantly suction, with values of $C_p=-1.4$ in the isolated tank and $C_p=-1.6$ in Configuration C_1. There are low suction values in C_1 at the junction with the cylinder. In the other Configurations C_2–C_5, peak pressures occur at the center of the cylinder (close to $0.5H$) with maximum values that are lower than in C_1.

Because it is difficult to appreciate details and differences in a three-dimensional representation, more detailed two dimensional plots are discussed next. Plots of pressure coefficients are summarized for the cylinder at elevations $0.50H$ and $0.90H$, considering all five configurations at $S=D$ in Fig. 6, together with results for the isolated tank. The results shown are not perfectly symmetric because of experimental deviations, but no averaging has been made in order to present the original results.

Pressures on the roof are plotted in Fig. 7 for the intersection of the roof with a plane passing through the windward meridian. Pressures are negative with the exception of small zones with low positive pressures at leeward.

Pressure distributions in elevation are represented in Fig. 8 at three meridians: windward meridian; the meridian facing the blocking tank in the windward region and the meridian at 180° from the previous one.

In most configurations the C_p values are higher than those in the isolated tank, considering both positive and negative pressures. The most severe changes are detected for the tandem configuration C_1, both in pressure patterns and values. For this configuration the flow passing the first tank produces stagnation

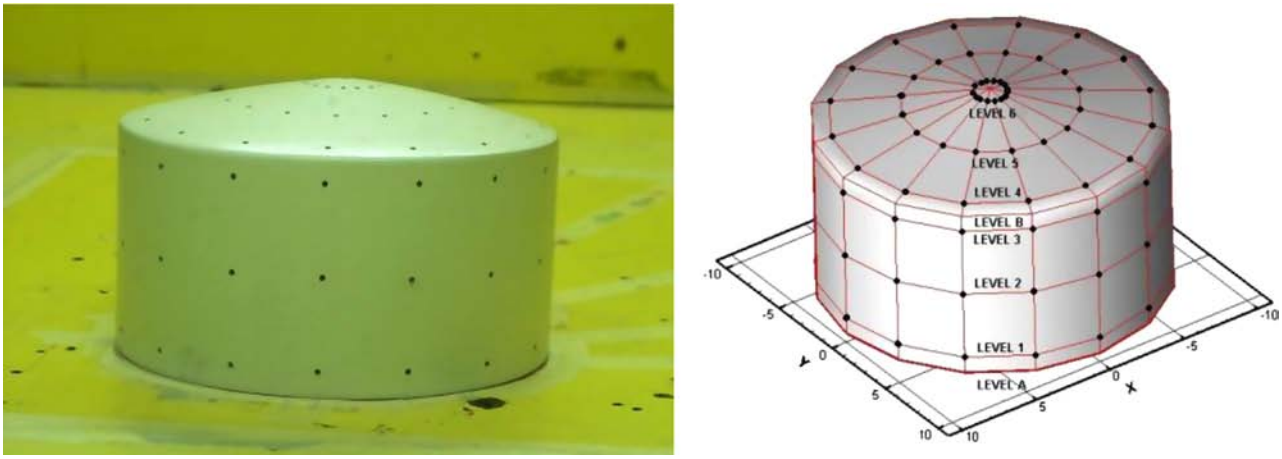

Fig. 3. Model tested with pressure gauges.

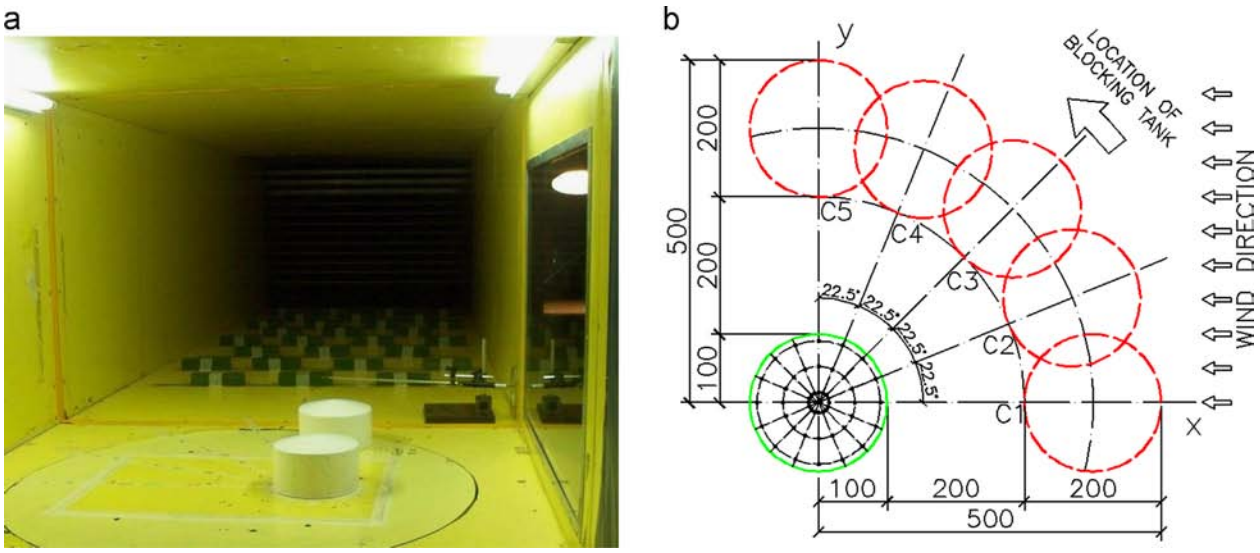

Fig. 4. (a) Test with a tank shielding a target tank and (b) configurations tested.

pressures on the target tank at an elevation closer to the joint with the roof. This effect was also observed in Ref. [13].

As the blocking tank is displaced to one side in Configurations C_2–C_4 the pressure pattern resembles the pattern in the single tank. In the leeward region, pressures are not so significantly modified, except for Configuration C_1 in which they are smaller.

The results in Fig. 8c indicate that on the meridian opposite to the blocking tank, the pattern of pressures are similar to the isolated tank but with higher values of suction.

For larger separations $S=1.5D$ and $S=1.8D$, the pressures are similar between them and approach the case with $S=1.0D$, but with lower positive and negative pressure coefficients. This is shown in Fig. 9 at elevation $0.90H$ (close to the joint with the roof), in which case the group effect is still different from the isolated configuration.

The three-dimensional pressures for tandem (C_1) and parallel (C_5) configurations have been plotted in Fig. 10 for $S=1.8D$. If the target tank is located further away from the blocking tank, then pressures decrease between 20% and 5% with respect to $S=1.0D$. Positive pressures increase by at least 15% and negative pressures by 25% with respect to the single tank.

3.2. Flow visualization and comparison with other studies

As mentioned before, the most relevant changes occur for the tandem configuration C_1, with pressures being higher than in the isolated tank and affecting the tank in the upper zone of the cylinder, where thicknesses are smaller.

To visualize the flow pattern, smoke was used in some wind tunnel tests for Configuration C_1 at $S=1.0D$. A typical photograph depicting the flow for a Configuration C_1 at $S=1.0D$ is shown in Fig. 11a, whereas the flow for the isolated tank is represented in Fig. 11b.

Because of the conical shape of the roof of the first tank, the stream lines become attached to the roof and then follow an initially descendent path between the two adjacent tanks. This is shown in the smoke tests in Fig. 11a by means of dotted lines which approximate the stream lines. As the flow passes the first tank, there is a wake which is characterized by low pressure and a vortex being generated which produces a change in the stream lines that arrive at the second tank. For a separation $S=1.0D$, the stream lines elevate as they approach the target tank.

The vortex modifies the pressures on the windward region of the target tank, with a shift in maximum pressures to a higher elevation (closer to the junction between the cylinder and the roof) than in the isolated tank. This is a change in the flow conditions between the isolated tank (C_0) and the tandem configuration (C_1), because in the former (Fig. 11b) the stream lines affect the central region at windward.

This effect is not the same as what has been previously observed by other authors in tandem configurations in which the first tank has a fixed roof. Results by Portela and Godoy [13] for a configuration with $S=1.0D$ but in which the first tank has a flat roof indicate that the flow passing the first tank tends to generate stream lines which follow the direction of the flat roof without inducing a descent between the two tanks. The first tank in this case shields the flow to the second tank, thus reducing the pressures on the target tank. Comparisons with tests by Sabransky and Melbourne [19] are not meaningful because those authors considered two tanks at very short spacing ($S=0.25D$), in which case the nature of the flow is completely different.

Although the effect shown in Fig. 11 has not been shown before in the context of oil storage tanks, this change in the position of stream lines and flow acceleration is commonly observed when flow passes a mountain and induces a wave on the lee of the mountain [21]; depending on the downstream location of a second object there may be an increase in pressures, as found for some configurations studied in the present research.

4. Bifurcation buckling of tanks under wind

4.1. Finite element model of the target tank

The stability analysis of shells has been more or less standardized thanks to the European Recommendations of Ref. [18]. Based on the general purpose finite element code ABAQUS [1], the structural response of the tanks has been computed in this work using bifurcation analysis (LBA) and geometrically nonlinear analysis with imperfections, GNIA.

The cylindrical shell was discretized by use of 8-node doubly-curved elements identified as S8R5, with reduced integration, whereas 6-node triangular elements with five degrees of freedom per node (element STRI65) were used for the roof. The mesh (some 10,000 elements) was defined by means of convergence studies.

The tank was designed according to API 650 [2] requirements, considering ASTM A-36 steel ($E=211$ GPa, $\nu=0.3$). Values of the

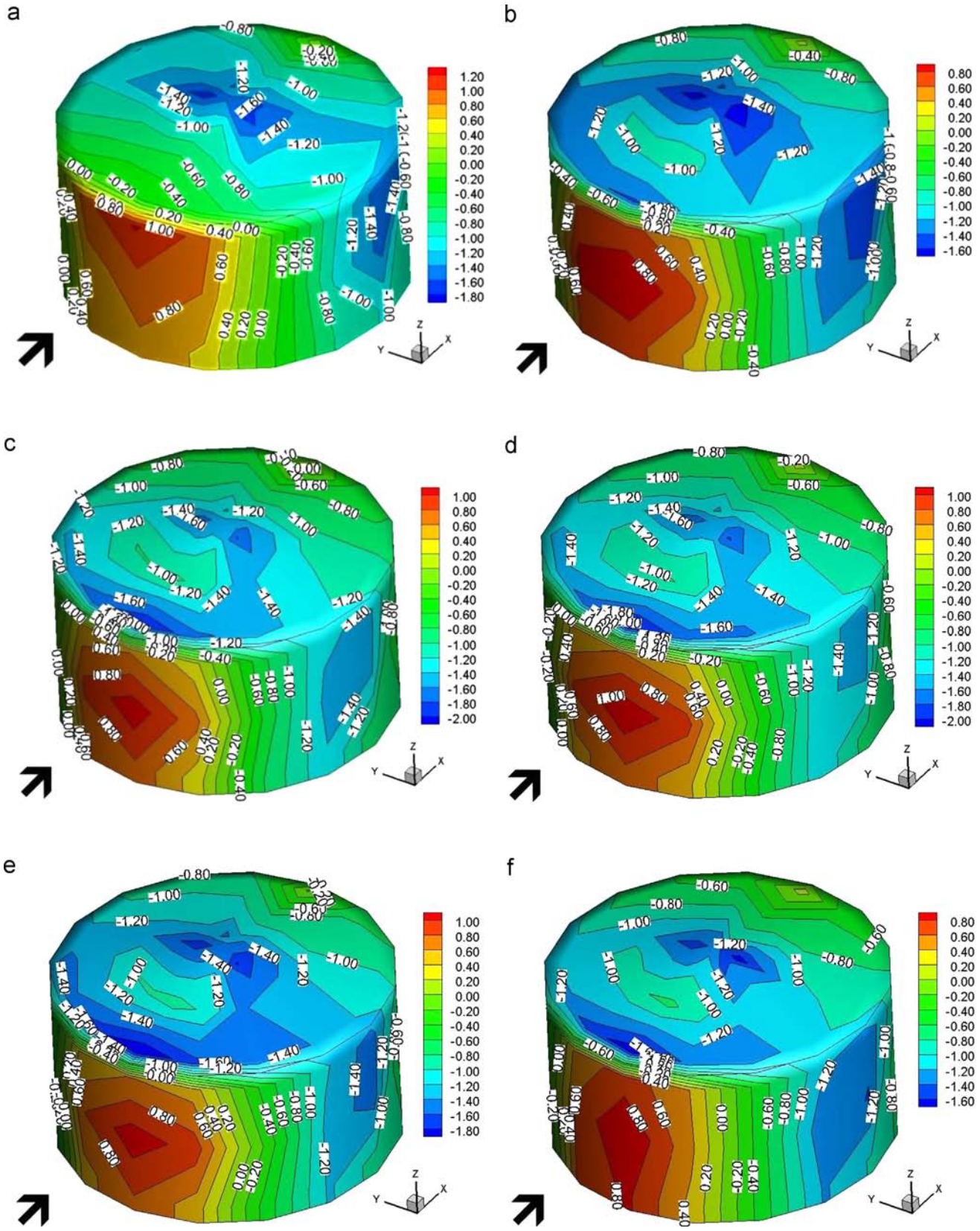

Fig. 5. Pressure coefficients for tanks with $S=1.0D$: (a) Configuration 1; (b) Configuration 2; (c) Configuration 3, (d) Configuration 4, (e) Configuration 5 and (f) isolated tank.

resulting thicknesses are shown in Table 2. The roof is assumed as a self-supported shell, but with a larger equivalent thickness, equal to three times the thickness in the thinnest course. This simplification has been used in a number of investigations based on equivalence between the stiffness of a roof with rafters supporting a thin shell and a thicker shell with uniform thickness and without rafters. Because relative values are of interest in this work to compare isolated tanks with two tank configurations, using the

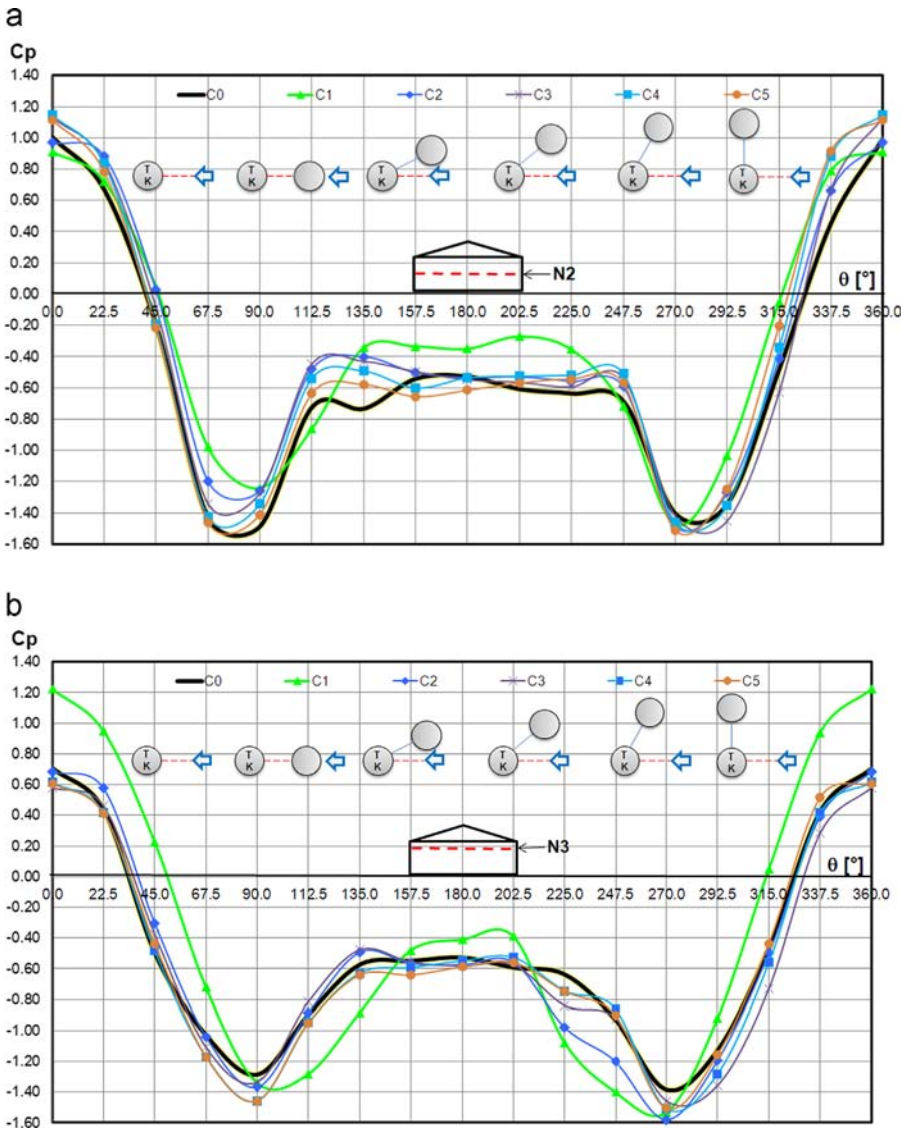

Fig. 6. Pressure coefficients around the circumference: (a) Elevation 2 (0.5*H*) and (b) Elevation 3 (0.9*H*).

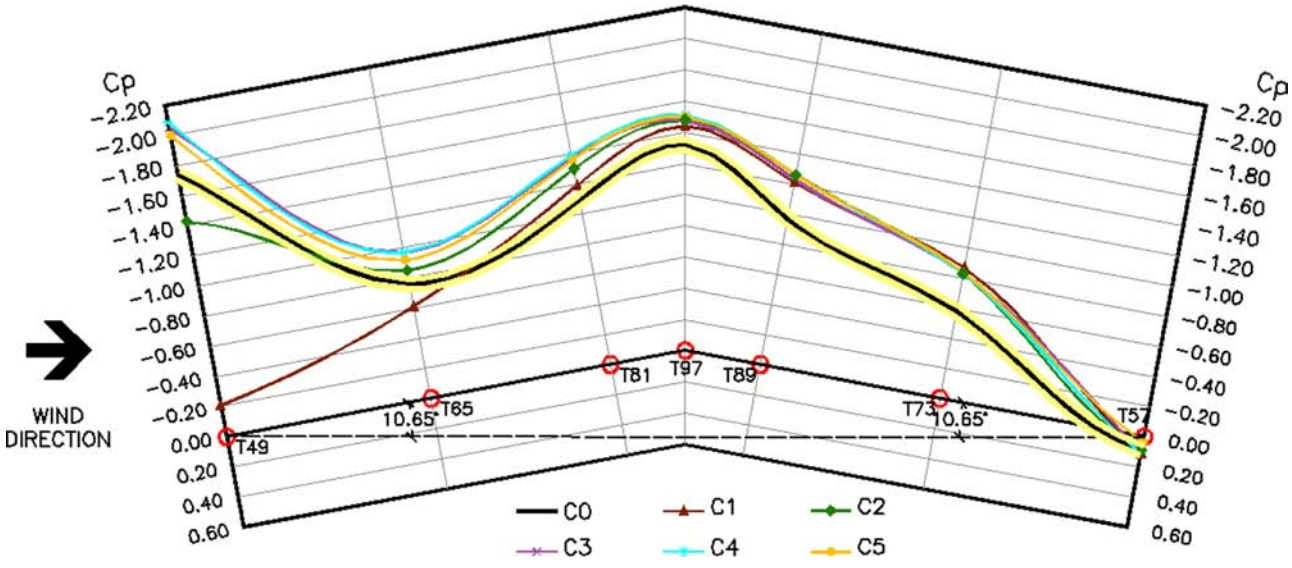

Fig. 7. Pressure coefficients on the roof.

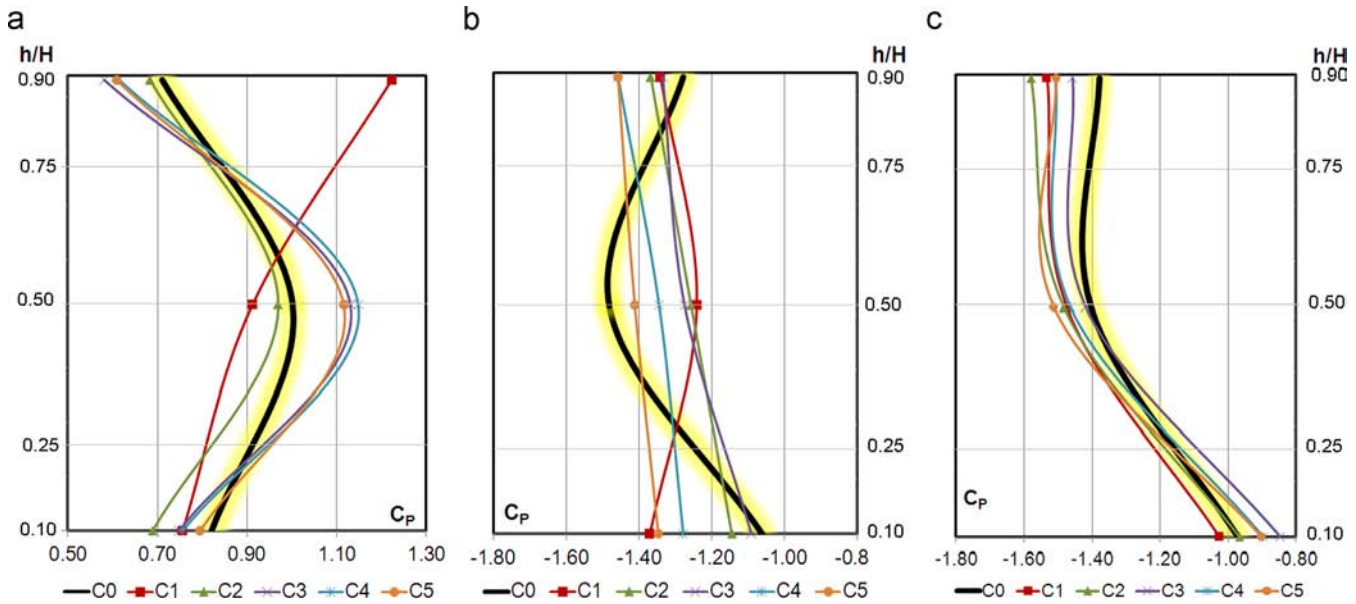

Fig. 8. Pressure coefficients in elevation: (a) windward meridian; (b) normal to wind direction, facing the blocking tank and (c) normal to wind direction, on the side opposite to the blocking tank.

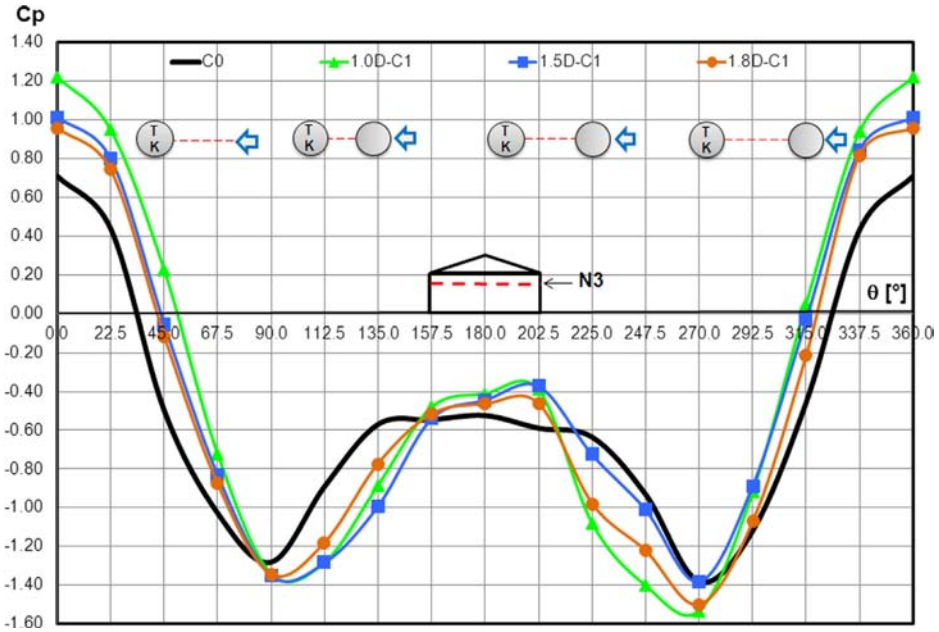

Fig. 9. Pressure coefficients around the circumference, at elevation 0.90*H*.

same simplification in both cases does not seem to produce great harm on the conclusions.

4.2. Linear bifurcation analysis, LBA

Wind pressure coefficients measured in the tests were employed as the basic pressure patterns and were scaled by a load factor λ in the LBA strategy to identify classical critical values λ_c and their associated eigenmodes. As shown in the literature [26], buckling of the shell is entirely dependent on the region of positive pressures at windward, and is only marginally affected by suction at other locations around the circumference.

A summary of LBA results is shown in Fig. 12a considering the lowest five eigenvalues in all studied configurations. Eigenvalues are obtained in pairs, due to a shift in the wave pattern. The eigenmode for C_1 and $S=1.0D$ is shown in Fig. 12b, with a shape which is very similar to what is computed for an isolated tank. The mode deflections are restricted to the windward region in the target tank and the rest of the tank remains unaffected at bifurcation buckling. The main difference is that the buckled region is displaced toward the top of the tank, where maximum pressures were measured in the wind tunnel tests.

In the isolated tank, the lowest eigenvalue was $\lambda_c=2.38$ kPa, while $\lambda_c=1.65$ kPa was computed in the most significant group effect (Configuration C_1, $S=1.0D$), leading to a reduction of 30%.

Bifurcation results are only an approximation to the buckling behavior of a shell and more refined GNIA studies are reported in the next section.

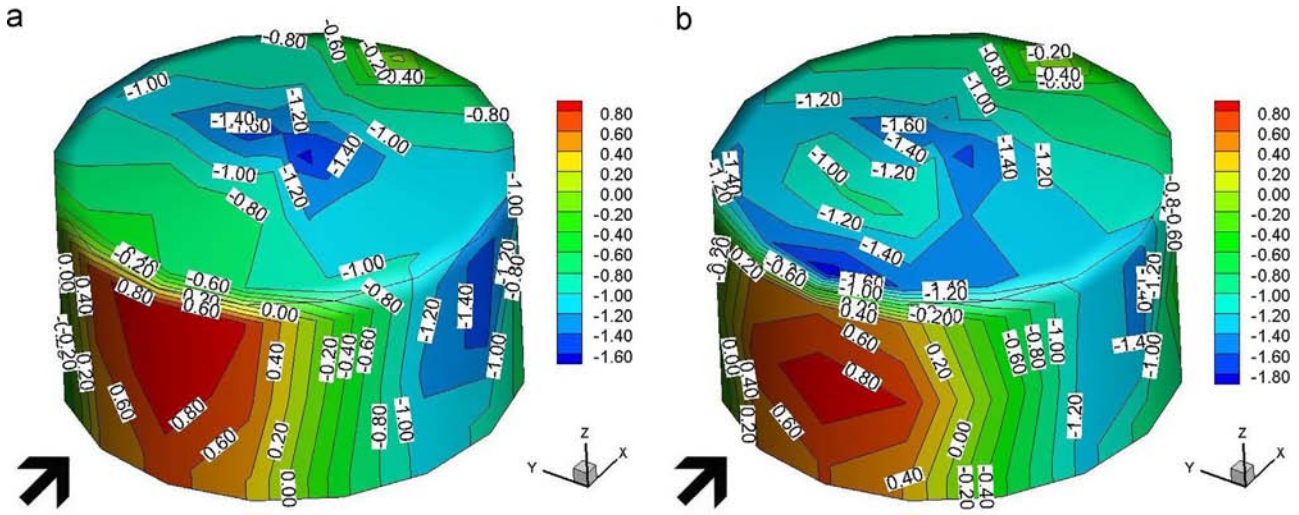

Fig. 10. Pressure coefficients for tanks at $S=1.8D$: (a) Configuration C_1 and (b) Configuration C_5.

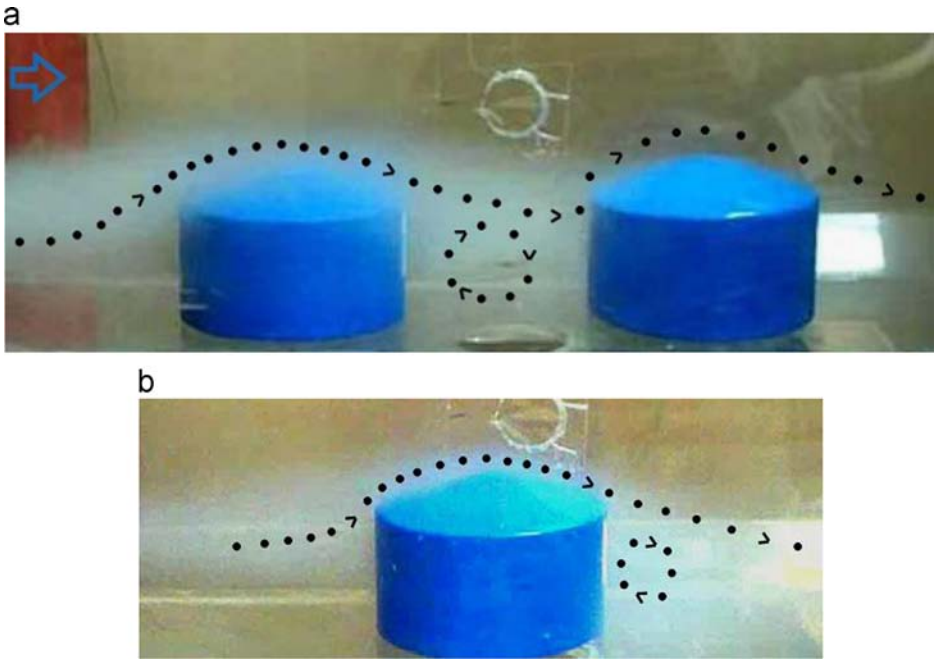

Fig. 11. Flow visualization: (a) tandem Configuration C_1 at $S=1.0D$ and (b) isolated tank.

5. Geometrically nonlinear analysis with imperfections, GNIA

5.1. Imperfections in the form of the lowest eigenvalue

The same finite element models as in LBA were used in the GNIA studies, in this case following the nonlinear equilibrium path by means of an algorithm due to Riks [16,17]. Eigenmode-affine imperfections (i.e., geometric imperfections having the same shape as the eigenmodes in LBA) were used. The amplitude ξ of the imperfection was assumed as $\xi=0.5t$, $\xi=0.75t$, and $\xi=1.0t$, where t is the thinner course thickness (top course in the cylindrical shell).

Equilibrium paths for the isolated tank and for Configurations C_1, C_2, and C_5, and for C_1 at $S=1.5D$ and $S=1.8D$, have been plotted in Fig. 13. The overall shape of the equilibrium path is the same in all cases, but the results are different depending on the configuration and imperfection amplitude considered.

For imperfection amplitudes $\xi<t$ there is a clear maximum load in the equilibrium path, but for $\xi=t$ in most cases the maximum is lost and the problem becomes one of large displacements rather than buckling. As expected, the most severe drop occurs for Configuration C_1, even for larger values of S. Differences between C_5 and the isolated tank are not so significant.

Curves of imperfection-sensitivity (maximum load in an equilibrium path vs. imperfection amplitude) are shown in Fig. 14: all curves have similar trends but at different values of maximum loads. Thus, the sensitivity slope is seen to be the same as in the isolated case C_0.

A summary of results for LBA and GNIA studies (for $\xi=0.75t$) is given in Table 3 for all configurations considered. The ratio between GNIA and LBA indicates that results with imperfections are lower than bifurcation loads. The most severe reductions in LBA critical loads occur for the Configuration C_1, in which the tanks are aligned with the direction of wind, with the reduction being

less pronounced as the distance S between tanks increases. A similar trend was found for GNIA studies.

5.2. Influence of imperfection shape on GNIA results

Eigenmode-affine imperfections investigated in the previous section were limited to shapes associated with the lowest eigenvalue in LBA study. This shape is the most detrimental imperfection in the vicinity of the critical state (as shown by Koiter [9]); however, for large imperfection amplitudes there is no certainty that higher eigenmodes do not produce ever more stringent reductions in maximum loads.

To evaluate effects due to the shape of imperfections, the first 100 eigenmodes have been considered and results are discussed in this section for isolated as well as for two tank configurations. Eigenmodes for the isolated tank are shown in Fig. 15: the largest displacements in mode 1 (M1) occur in the cylinder at the windward region; most lower modes are similar with variations in the number of circumferential waves and their extent. Fig. 15b shows the first mode with significant roof deflections, M15.

For two-tank Configuration C_1, the modes are shown in Fig. 16 for $S=1.0D$. The lowest modes (Fig. 16a, b, and e) have displacements in the windward region; a roof mode is shown in Fig. 16c, whereas mode M23 (Fig. 16d) has displacements in the leeward region.

To evaluate equilibrium paths, imperfection amplitudes $\xi=0.75t$ were considered because this is the imperfection for which the most severe reductions in maximum loads are obtained before a maximum is lost. Results for the isolated tank are given in Fig. 17: only a limited number of cases are plotted in this figure. Modes have been taken in isolation or in combinations of two modes to include cylinder and roof displacements. There is a slight reduction in maximum load for imperfection shape M1+M15 with respect to mode M1, as shown in Fig. 17 and Table 4; however, the difference is of only 1.7%.

Table 2
Thickness of the cylindrical shell.

Course	Elevation (m)	Thickness	
		(m)	(in.)
1	1.50	0.0191	3/4
2	3.00	0.0159	5/8
3	4.50	0.0143	9/16
4	6.00	0.0127	1/2
5	7.50	0.0127	1/2
6	9.00	0.0095	3/8
7	10.50	0.0079	5/16
8	12.00	0.0063	1/4
9	13.50	0.0063	1/4
10	15.00	0.0063	1/4
11	15.75	0.0063	1/4

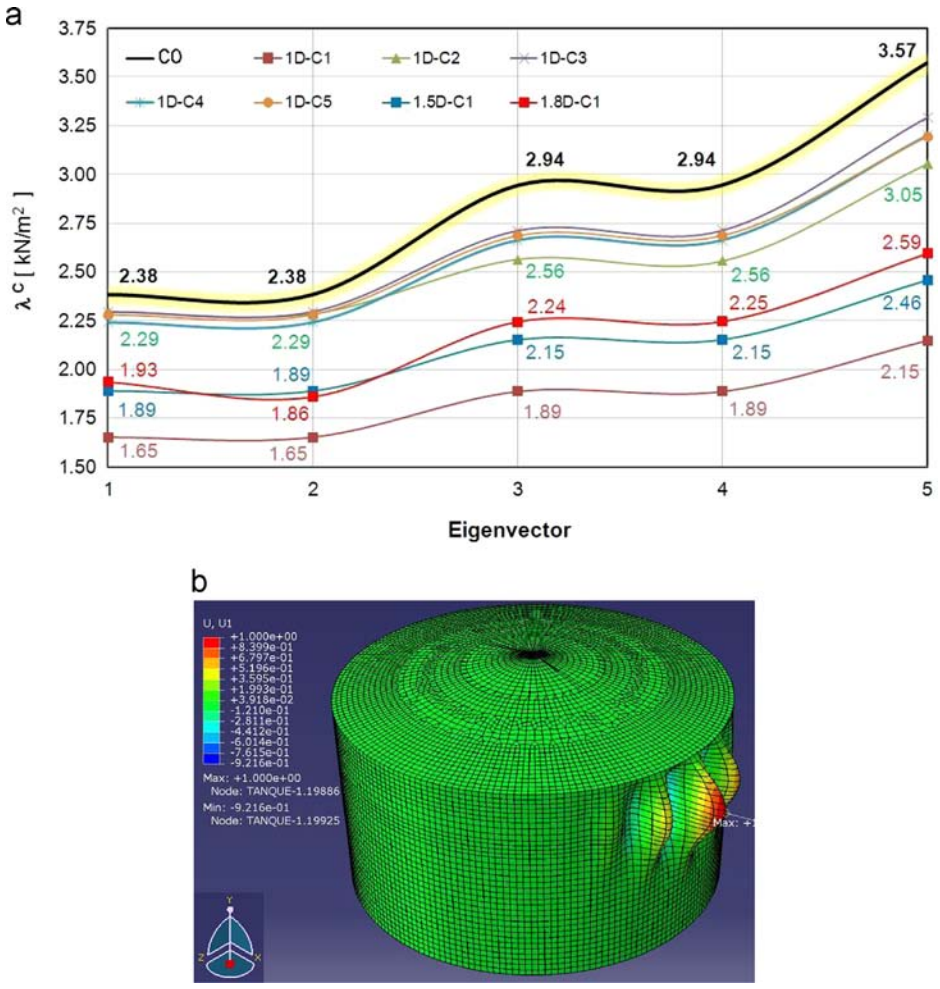

Fig. 12. LBA results: (a) critical loads for the lowest five eigenvalues and (b) first mode ($\lambda^C=1.65$ kN/m^2), Configuration C_1 at $S=1.0D$ (indicated as 1D-C1 in (a)).

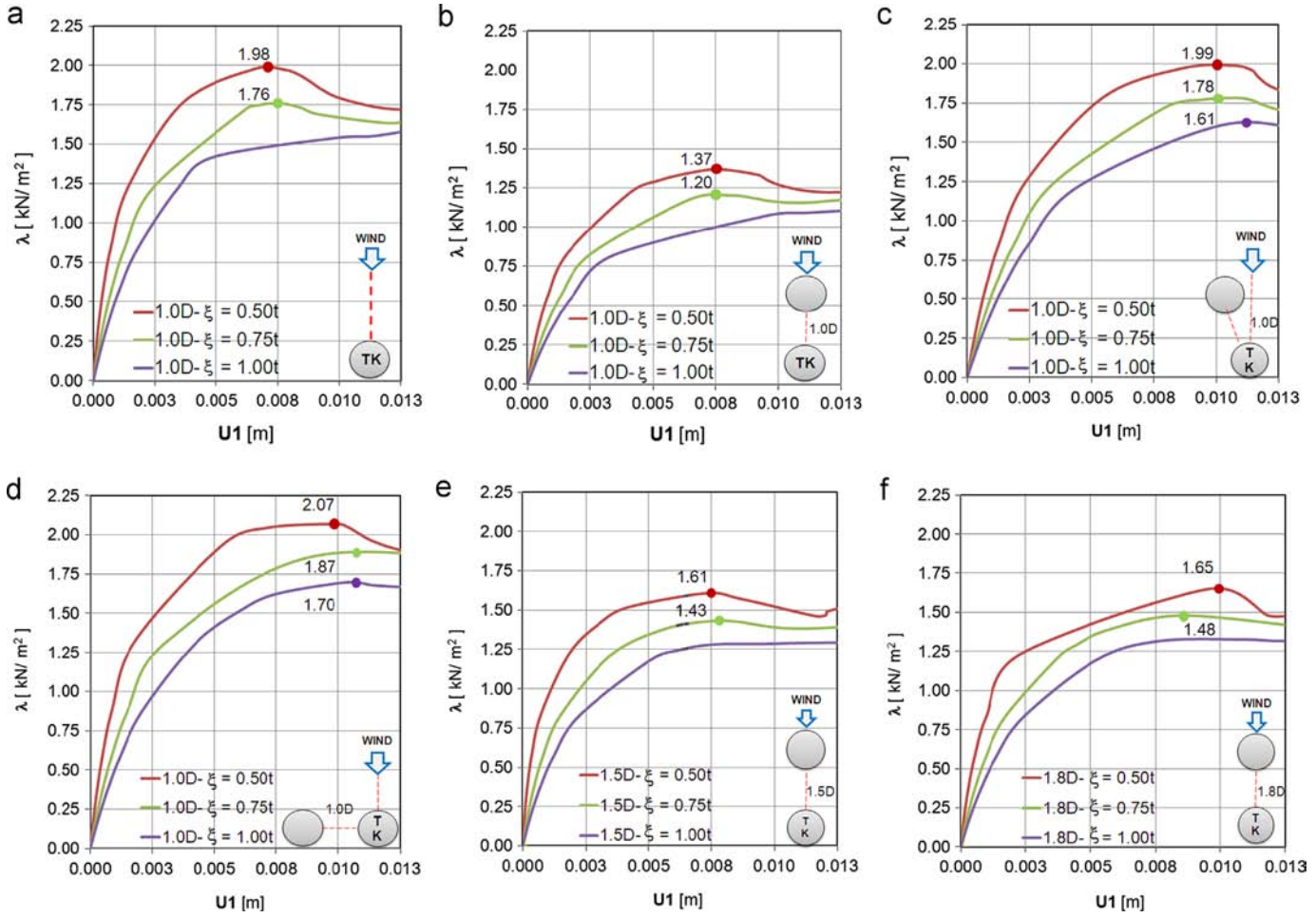

Fig. 13. Equilibrium paths: (a) isolated tank; (b) Configuration C_1 at $S=1.0D$; (c) Configuration C_2 at $S=1.0D$; (d) Configuration C_5 at $S=1.0D$; (e) Configuration C_1 at $S=1.5D$ and (f) Configuration C_1 at $S=1.8D$.

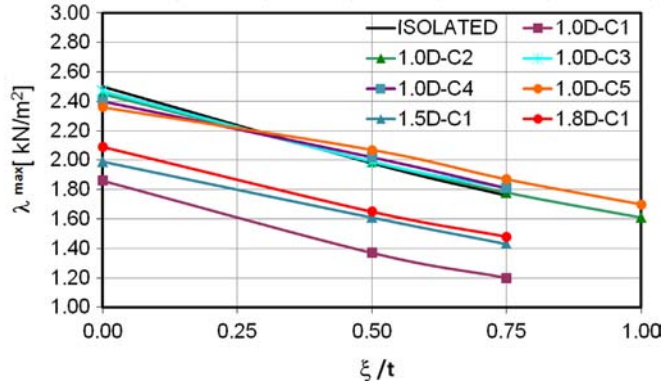

Fig. 14. Imperfection-sensitivity diagram for isolated tank and five configurations considered.

For two tanks in Configuration C_1 separated at $S=1.0D$, results for imperfection shapes in the form of individual eigenmodes are shown in Fig. 18, assuming $\xi=0.75t$. The most detrimental case is mode M1.

Combinations of modes are shown in Fig. 19, for cylinder modes and roof modes. There are combinations that yield lower λ^{max} values but the differences with respect to mode M1 are of 1.5% (see Table 4).

Because of the minor effect of mode combinations on the maximum load in GNIA studies, it may be accepted that results based on the lowest eigenmode are a good approximation.

6. Conclusions

The pressure patterns due to wind on two tanks in tandem or skew arrangements have been identified in this work by means of wind tunnel testing. The configurations studied are simplified representations of wind tanks located on the perimeter of a tank farm, or in a second line in which a tank is shielded by another tank placed in the perimeter.

The results show significant differences between a tandem configuration (both tanks aligned with the wind direction) and an isolated tank, with peak pressures on the windward meridian being at a higher elevation (closer to the roof), and with increases in pressure coefficients. An increase in suctions is also found on the roof. The differences with the isolated tank become less important as the angle of wind incidence increases, and in the limit the two tanks that are in line perpendicular to wind have the lesser effect.

The pressures accounting for two tank interaction were next used in a finite element analysis of shell buckling and post-buckling. Group effects are reflected in both, bifurcation LBA and geometrically nonlinear analysis with imperfections GNIA studies.

Table 3
Critical load factors (λ^c, LBA) and maximum loads (λ^{max}, GNIA) for several configurations (ξ=0.75t).

	Isolated tank	S=1.0D					S=1.5D	S=1.8D
		C_1	C_2	C_3	C_4	C_5	C_1	C_1
LBA								
λ^c [kPa]	2.38	1.65	2.29	2.30	2.24	2.28	1.89	1.93
$\lambda^c/\lambda^c_{\text{isolated}}$	–	0.69	0.96	0.96	0.94	0.96	0.79	0.81
GNIA								
λ^{max} [kPa]	1.76	1.20	1.61	1.81	1.81	1.70	1.43	1.48
$\lambda^{max}/\lambda^{max}_{\text{isolated}}$		0.68	0.91	1.03	1.03	0.96	0.81	0.84
GNIA vs. LBA								
λ^{max}/λ^c	0.74	0.73	0.70	0.79	0.81	0.75	0.76	0.77

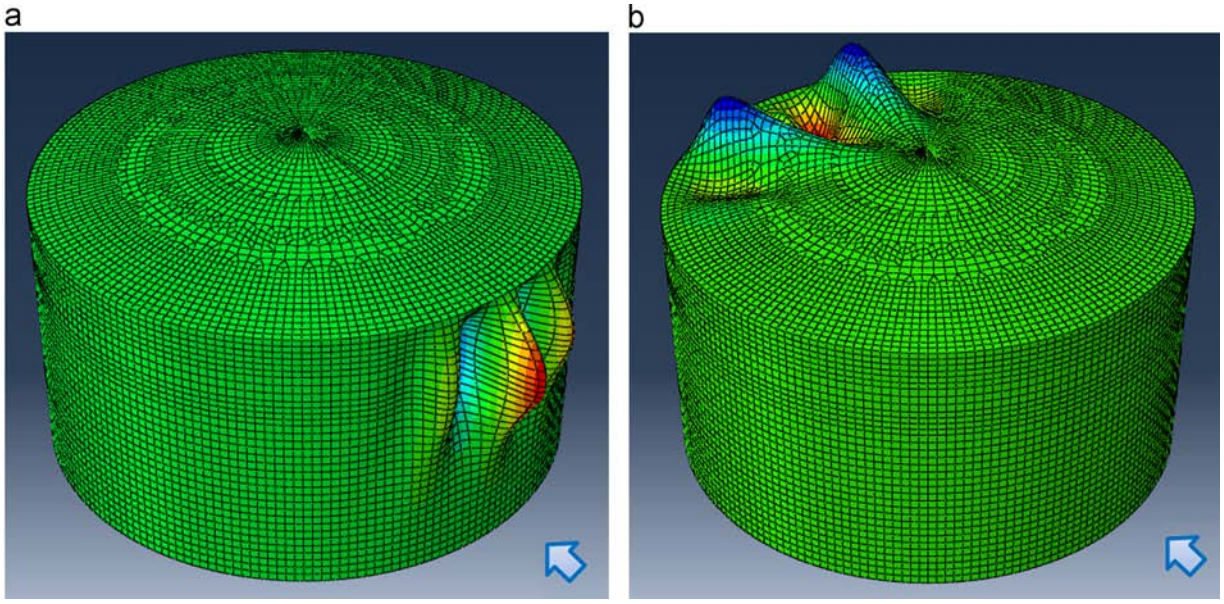

Fig. 15. Eigenmodes for isolated tank: (a) first mode (λ^C=2.38 kN/m^2) and (b) Mode 15 (λ^C=6.37 kN/m^2).

Maximum changes in buckling loads occur in the tandem configuration with tank separation of one diameter. The maximum reductions computed (tandem configuration) are of 30% in classical critical pressures (or in geometrically nonlinear analysis), with smaller changes (in the order of 5%) in other two-tank configurations. Reductions in buckling pressures of approximately 20% were found for tank separations of 1.5 and 1.8 times the diameter.

The shape of the imperfection considered in GNIA studies for the lowest 100 eigenvalues, indicate that the shape associated with the lowest eigenvalue yields good estimates of most severe imperfection sensitivity.

A correlation between pressure changes and buckling changes cannot be easily made, but in the present study there were 15% changes in pressures for tandem configurations, which induced changes of the same order in buckling loads as computed via LBA, and even larger drops (30%) in maximum loads via GNIA.

Because pressures and critical loads depend so heavily on the geometry of the blocking tank, results obtained for long cylinders do not provide useful information on this problem. Even data obtained for one type of roof cannot be generalized to another type.

There are limitations to draw general recommendations oriented to design based on case studies of limited tank arrangements, but some observations can be made at present which are of value to design and to understanding the safety of existing plants under wind loads.

The results presented in this paper, taken in conjunction with results by other authors for other groups of tanks considered, have some direct consequences for design. First, the most severe changes in pressures due to blocking of a tank by another one occur in a tandem configuration, for which two tanks are aligned with the wind direction. From the point of view of design, this cannot be anticipated because wind direction changes with respect to the arrangement of tanks in a tank farm. Second, there is an influence of the configuration of the front tank on pressures and buckling on the target tank. For a given tank arrangement, tandem configurations in which tanks in the periphery of a plant have a flat roof or do not have a fixed roof, the state of the art seems to indicate that no increase in pressures on the target tank will occur and the case of an isolated tank represents a lower bound to buckling loads. On the other hand, if tanks in the periphery have a conical roof (and this may extend to shallow dome configurations), then pressure increases at critical locations (top part of the cylinder, for which the thickness is small) should be expected, with the consequence that the case of an isolated tank may be an upper bound to buckling loads.

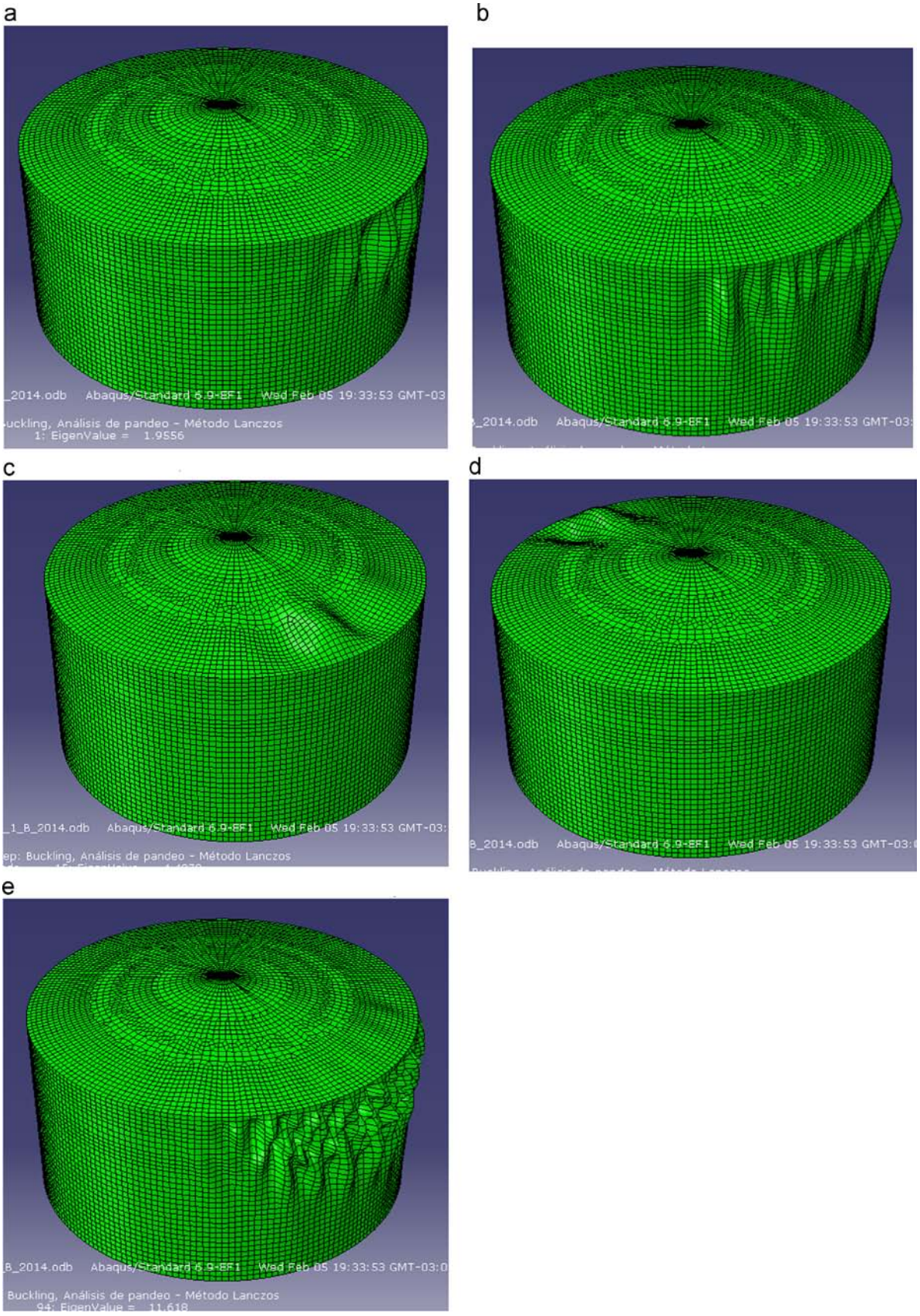

Fig. 16. Shape modes for Configuration C_1, $S=1.0D$: (a) first critical mode; (b) Mode 14; (c) Mode 15; (d) Mode 23 and (e) Mode 94.

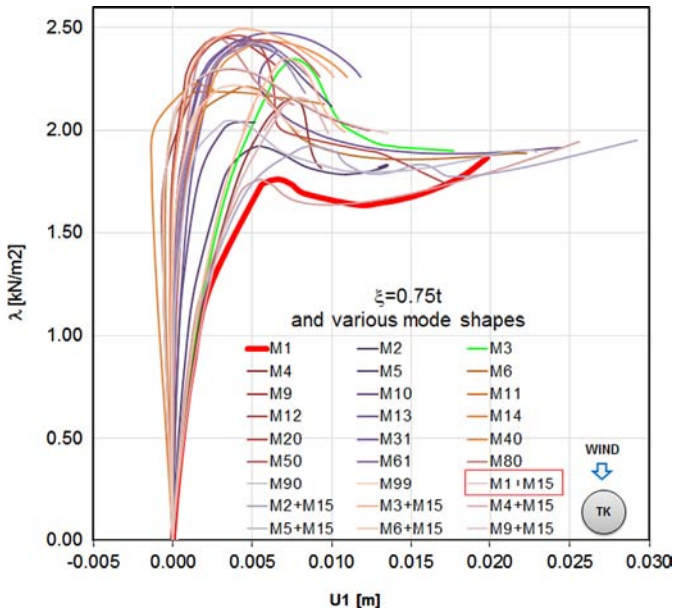

Fig. 17. Equilibrium paths for an isolated tank for imperfection amplitude $\xi=0.75t$ and various mode shapes.

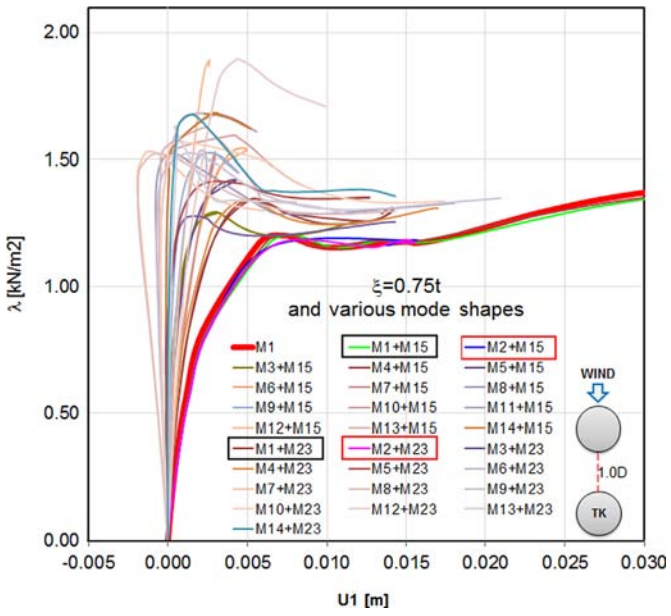

Fig. 19. Equilibrium paths for Configuration C_1, $S=1.0D$, for imperfection $\xi=0.75t$ and various imperfection shapes.

Table 4
Maximum loads obtained via GNIA (with $\xi=0.75t$) for Configuration C_1 with $S=1.0D$.

Eigenmode affine imperfection in mode M	Isolated tank		Two tanks at $S=1.0D$, C_1	
	λ^{max} [kN/m^2]	Difference [%]	λ^{max} [kN/m^2]	Difference [%]
M1	1.7582		1.2025	
M1+M15	1.7283	−1.70	1.2019	−0.05
M2+M15			1.1851	−1.45
M1+M23			1.2020	−0.04
M2+M23			1.1846	−1.49

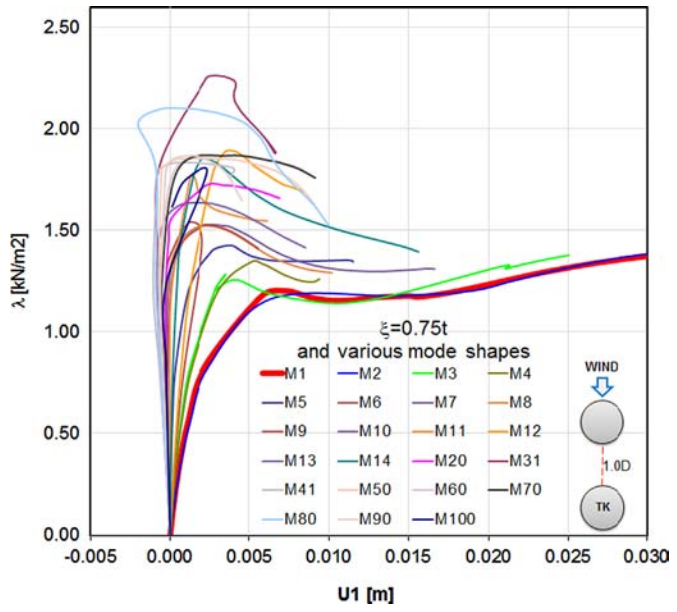

Fig. 18. Equilibrium paths for Configuration C_1, $S=1.0D$, for imperfection amplitude $\xi=0.75t$ and various imperfection shapes.

Acknowledgments

The authors thank Dr. Sebastián Delnero, Dr. Jorge Colman-Lerner, Dr. Julio Marañón-DiLeo, and Mariano García, members of the Boundary Layer and Fluid Dynamics Lab at the National University of La Plata in Argentina, for their help during the tests. RCJ thanks the support during this research received through grants from the National University of Comahue (SECYT-UNCo). LAG thanks the support received through grants from the National University of Cordoba (SECYT-UNC) and CONICET (PIP 112-201201-00126-CO).

References

[1] ABAQUS. User's manuals. Rhode Island, USA: Hibbitt, Karlsson and Sorensen, Inc.; 2006.
[2] API. Standard 650: welded steel tanks for oil storage. Washington, DC: American Petroleum Institute; 2010.
[3] ASCE 7 Standard. Minimum design loads for building and other structures. Reston, VA, USA: American Society of Civil Engineering; 1999.
[4] Esslinger M, Ahmed S, Schroeder H. Stationary wind loads of open topped and roof-topped cylindrical silos. Der Stahlbau; 1971. p. 1–8.
[5] Eurocode 3. Design of steel structures – Part 4-2: tanks. Brussels: European Committee for Standardization; 2007.
[6] Gu Z, Sun T. Classifications of flow pattern on three circular cylinders in equilateral-triangular arrangements. J Wind Eng Ind Aerodyn 2001;89:553–68.
[7] Iamandi C, Georgescu A, Erbasu C. Experimental modeling of a four steel tanks battery. In: Proceedings of the 11th international conference on wind engineering. Lubbock (Texas, USA); 2003.
[8] Jaca RC. Lower bounds to shell instability in thin-walled tanks [Ph.D. thesis]. Córdoba, Argentina: National University of Córdoba; 2005 [in Spanish].
[9] Koiter WT. On the stability of elastic equilibrium [Ph.D. thesis]. Delft, Holland: Delft Institute of Technology; 1945 [in Dutch] [English translation by NASA, 1967].
[10] MacDonald PA, Kwok KC, Holmes JD. Wind loads on circular storage bins, silos and tanks – Part I: point pressure measurements on isolated structures. J Wind Eng Ind Aerodyn 1988;31:165–88.
[11] MacDonald PA, Holmes JD, Kwok KC. Wind loads on circular storage bins, silos and tanks – Part II: effect of grouping. J Wind Eng Ind Aerodyn 1990;34:77–95.
[12] Orlando M. Wind-induced interference effects on two adjacent colling towers. Eng Struct 2001;23:979–92.
[13] Portela G, Godoy LA. Shielding effects and buckling of steel tanks in tandem arrays under wind pressures. Wind Struct 2005;8(5):325–42.
[14] Portela G, Godoy LA. Wind pressures and buckling of aboveground steel tanks with a conical roof. J Constr Steel Res 2005;61(6):786–807.
[15] Portela G, Godoy LA. Wind pressures and buckling in grouped steel tanks. Wind Struct 2007;10(1):1–22.

[16] Riks E. An incremental approach to the solution of snapping and buckling problems. Int J Solids Struct 1979;15:529–51.
[17] Riks E. The application of Newton's method to the problem of elastic stability. J Appl Mech 1972;39:1060–5.
[18] Rotter JM, Schmidt H, editors. Buckling of steel shells: European design recommendations. 5th ed.. Mem Martins, Portugal: European Convention for Construction Steelwork; 2008.
[19] Sabransky IJ, Melbourne WH. Design pressure distribution on circular silos with conical roofs. J Wind Eng Ind Aerodyn 1987;26:65–84.
[20] Said NM, Mhiri H, Bournot H, Le Palec G. Experimental and numerical modelling of the three-dimensional incompressible flow behaviour in the near wake of circular cylinders. J Wind Eng Ind Aerodyn 2008;96:471–502.
[21] Scorer RS. Theory of waves in the lee of mountains. Q J Meteorol Soc 1949;75:41–56.
[22] Tsutsui T, Igarashi T, Kamemoto K. Interactive flow around two circular cylinders of different diameters at close proximity. J Wind Eng Ind Aerodyn 1997;67:279–91.
[23] Uematsu Y, Yasunaga U. Wind loads on open-topped oil-storage tanks in various arrangements. In: Proceedings of the sixth European and African conference on wind engineering. Cambridge, UK; 2013.
[24] Vickery BJ, Ansourian P. An investigation of the failure due to wind action of a group of six silos at Boggabri, NSW, Report S152. Sydney: School of Civil Engineering, University of Sydney; 1974.
[25] Yasunaga J, Koo C, Uematsu Y, Kondo K, Yamamoto M. Wind loads on two or three open-topped oil-storage tanks in various arrangements. In: Choi CK, editor. Proceedings of the world congress on advances in civil, environmental, and materials research. Seoul, Korea: Techno Press; 2012. p. 2339–52.
[26] Zhao Y, Lin Y. Buckling of cylindrical open-topped steel tanks under wind load. Thin-Walled Struct 2014;79:83–94.
[27] Zhao Y, Lin Y, Shen Y. Wind loads on large cylindrical open-topped tanks in group. Thin Walled Struct 2014;78:108–20.
[28] Zdravkovich MM. Review of flow interference between two cylinders in various arrangements. ASME J Fluids Eng 1977;99:618–33.